Supplementary Material (ESI) for Organic & Biomolecular Chemistry

One-pot Syntheses of Donor-Acceptor [2]Rotaxanes Based on Cryptand/Paraquat Recognition Motif

Zhikai Xu, Lasheng Jiang*, Yahui Feng, Suhui Zhang, Jidong Liang, Shaowu Pan, Yu Yang, Dengke Yang and Yuepeng Cai

School of Chemistry and Environment, South China Normal University, Guangzhou, 510631, P. R. China. Tel and Fax: +86-20-39310187; E-mail jianglsh@scnu.edu.cn

Supporting Information

Table of Contents

1. Benesi-Hildebrand plots for the association constants of **1a·3** and **1b·3** in CD_3CN

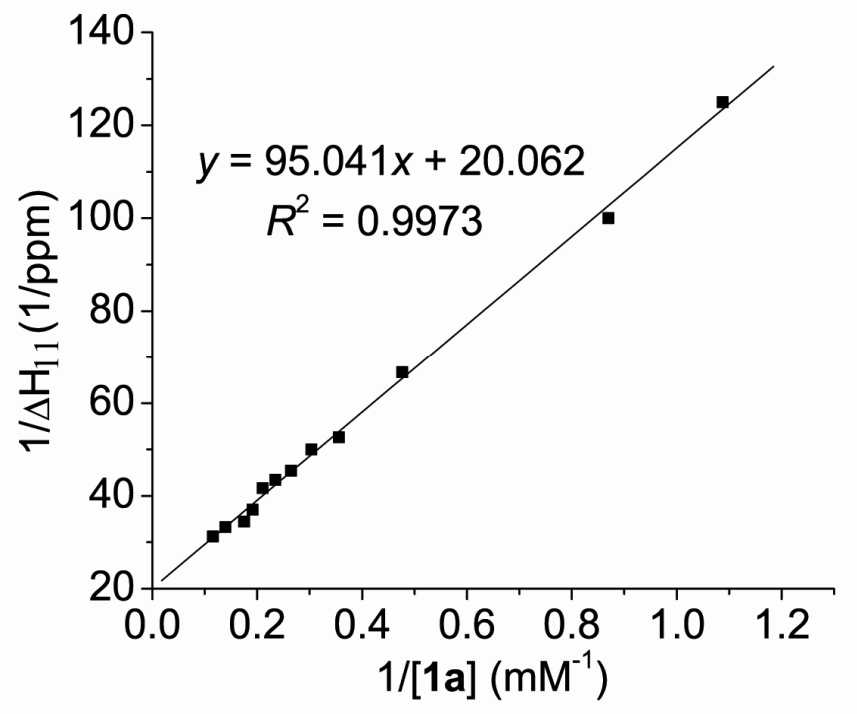

Figure S1 Benesi-Hildebrand plots for the formation of [2]pseudorotaxanes cryptand **1a** with paraquat derivative **3** based on the data for proton H_{11} at 22℃ in CD_3CN. $[\mathbf{3}]_0$ = 0.50 mM.

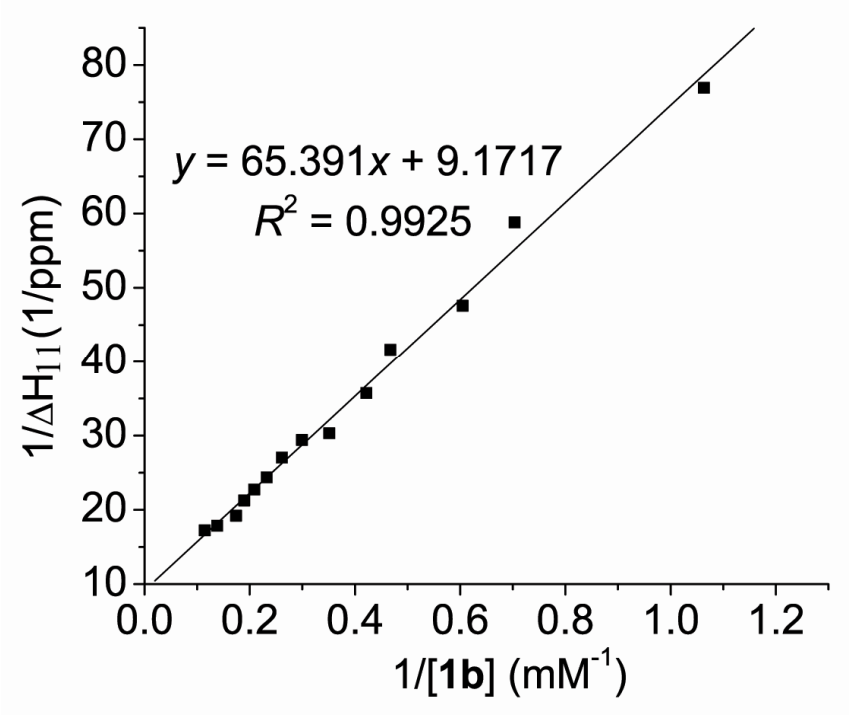

Figure S2 Benesi-Hildebrand plots for the formation of [2]pseudorotaxanes cryptand **1b** with paraquat derivative **3** based on the data for proton H_{11} at 22℃ in CD_3CN. $[\mathbf{3}]_0$ = 0.50 mM.

2. Mole ratio plots for determination of stoichiometry of complexation between cryptand **1a**/**1b** and paraquat derivative **3**

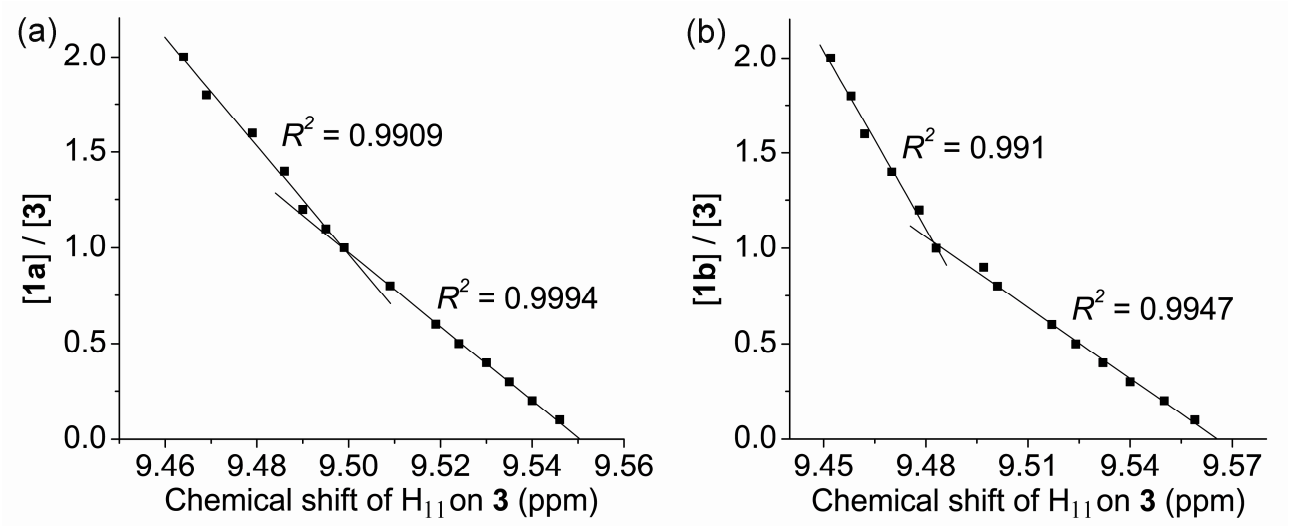

Figure S3 Mole ratio plots for determination of stoichiometry of complexation between (a) cryptand **1a** and paraquat derivative **3**, and (b) cryptand **1b** and paraquat derivative **3** in [D_6]acetone. [**3**]$_0$ = 2.00mM

3. Electrospray ionization mass spectra of host **1a**/**1b** with guest **3** in acetonitrile

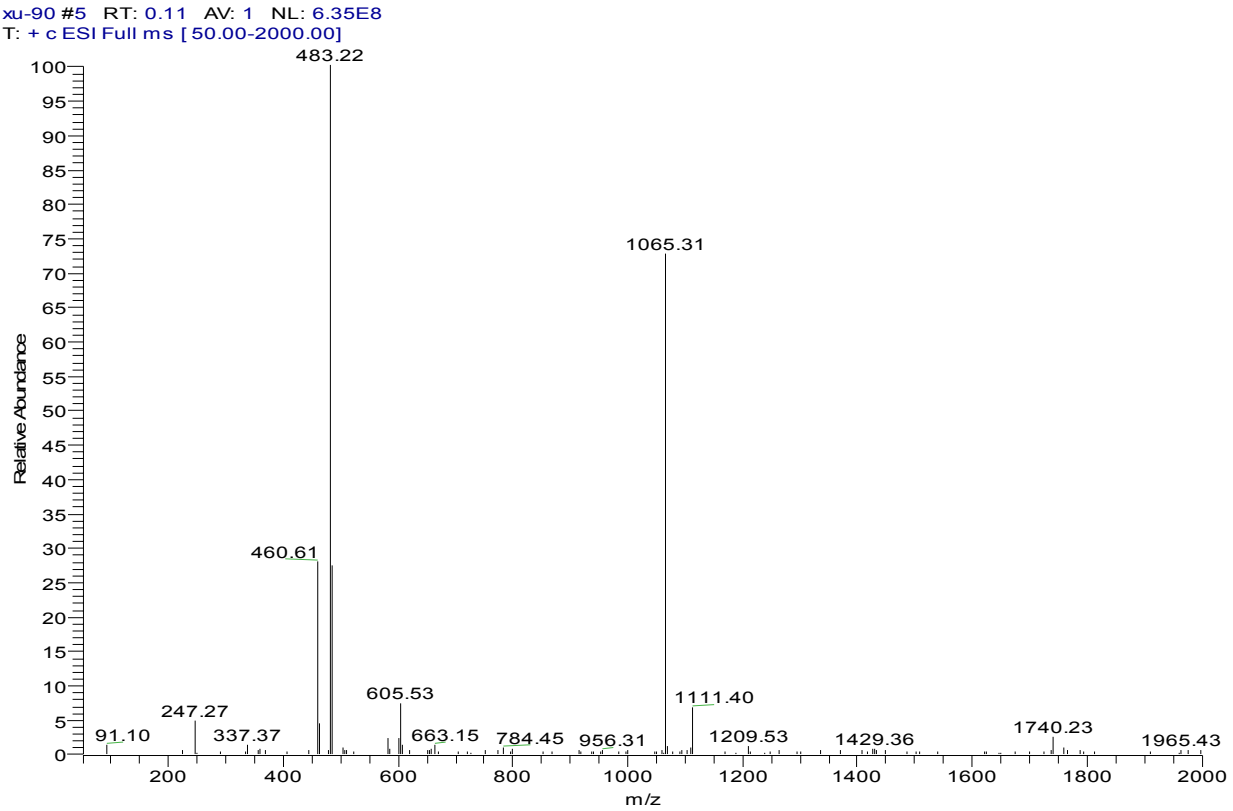

Figure S4 Low-resolution ESI-MS of [2]pseudorotaxane **1a**·**3** in acetonitrile

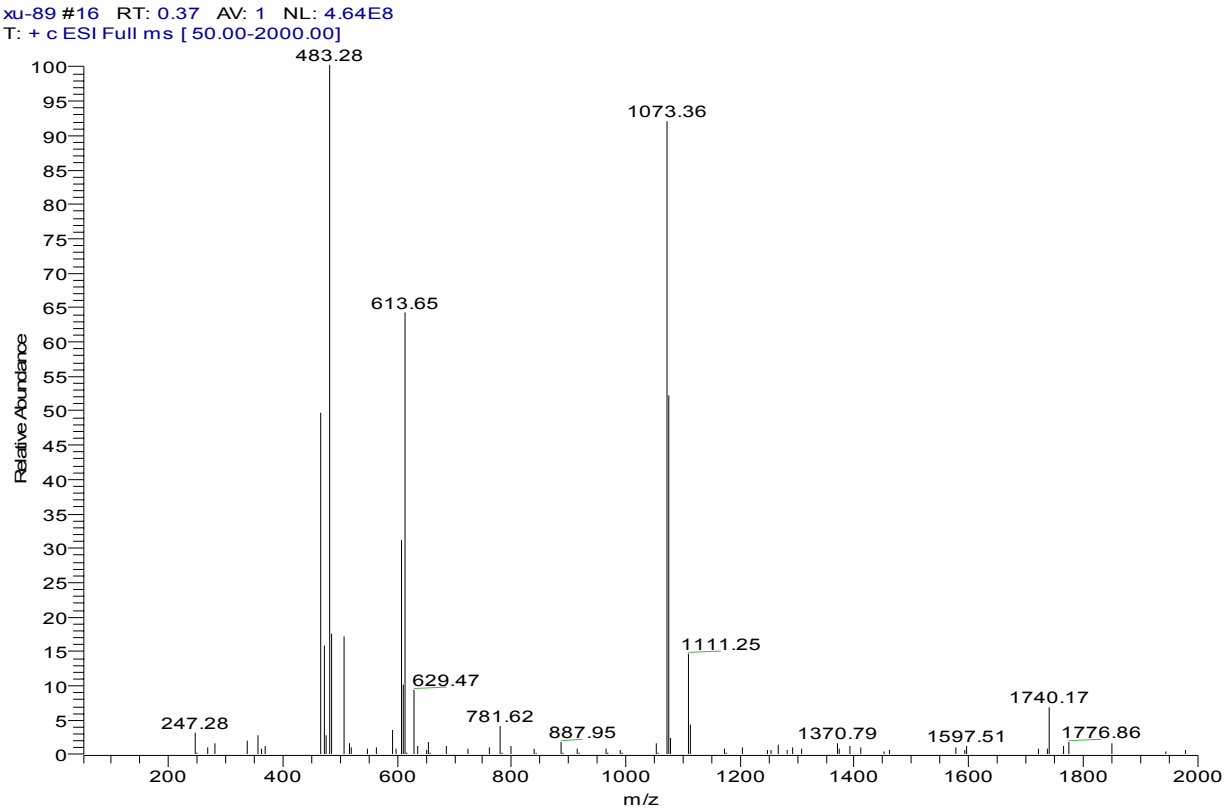

Figure S5 Low-resolution ESI-MS of [2]pseudorotaxane **1b·3** in acetonitrile

4. ^{1}H NMR and Low-resolution ESI-MS spectra of dumbbell-shaped compound **6**

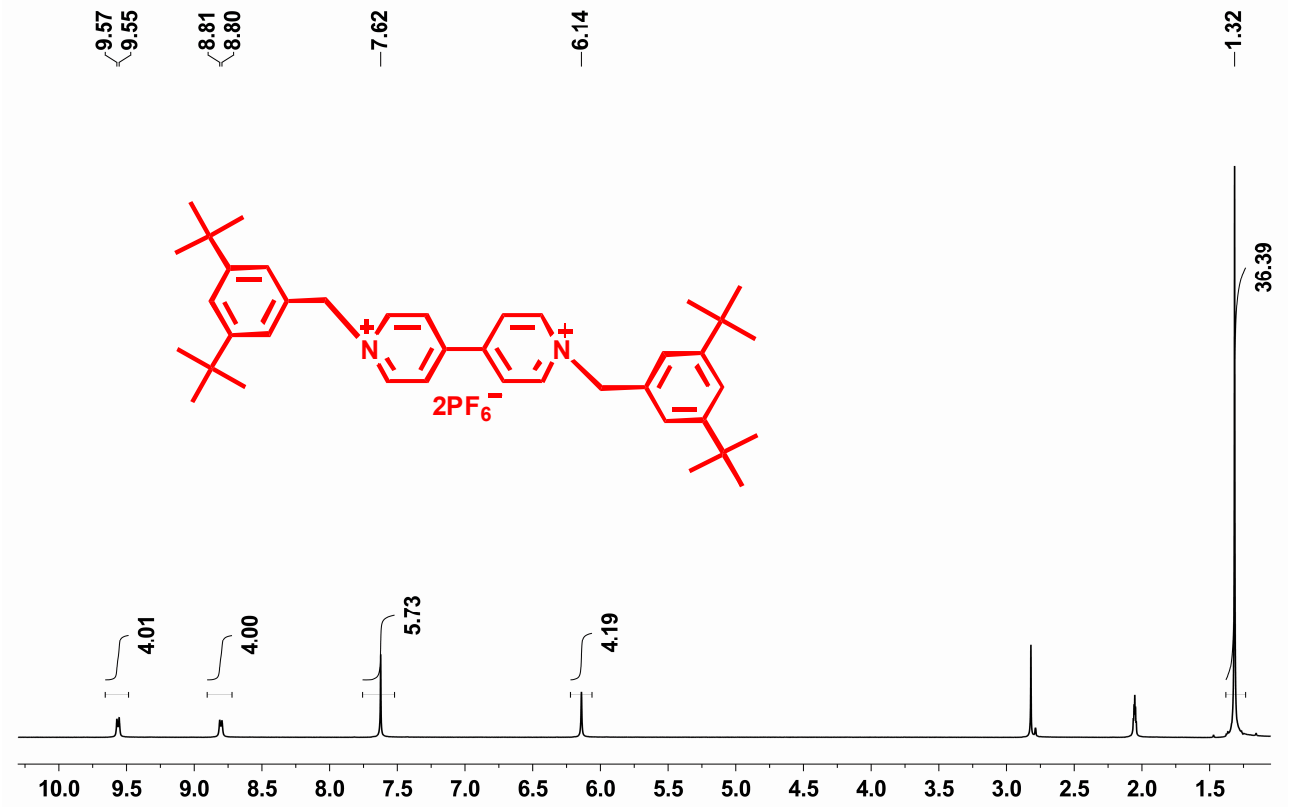

Figure S6 ^{1}H NMR spectrum (400MHz, CD_3COCD_3, 22℃) of dumbbell-shaped compound **6**

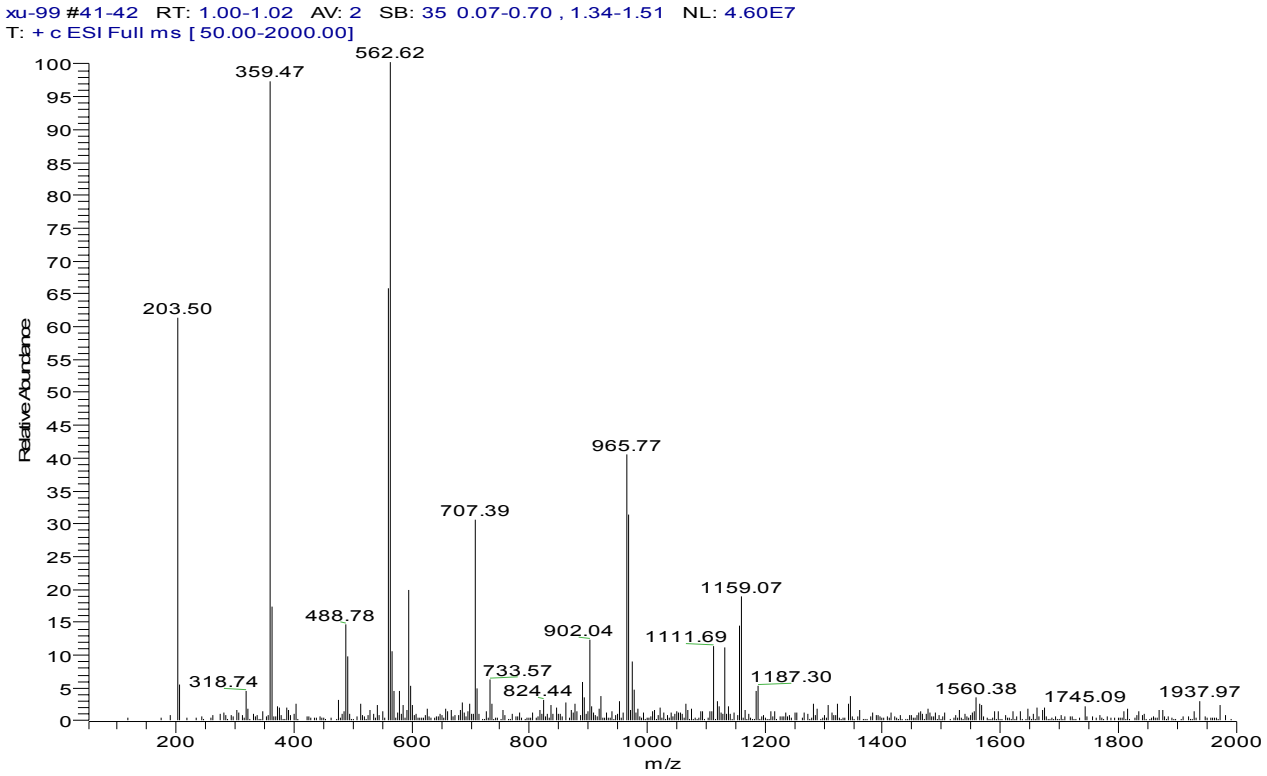

Figure S7 Low-resolution ESI-MS of dumbbell-shaped compound **6**

5. ^{1}H NMR and ^{13}C NMR spectra of [2]rotaxane **7**

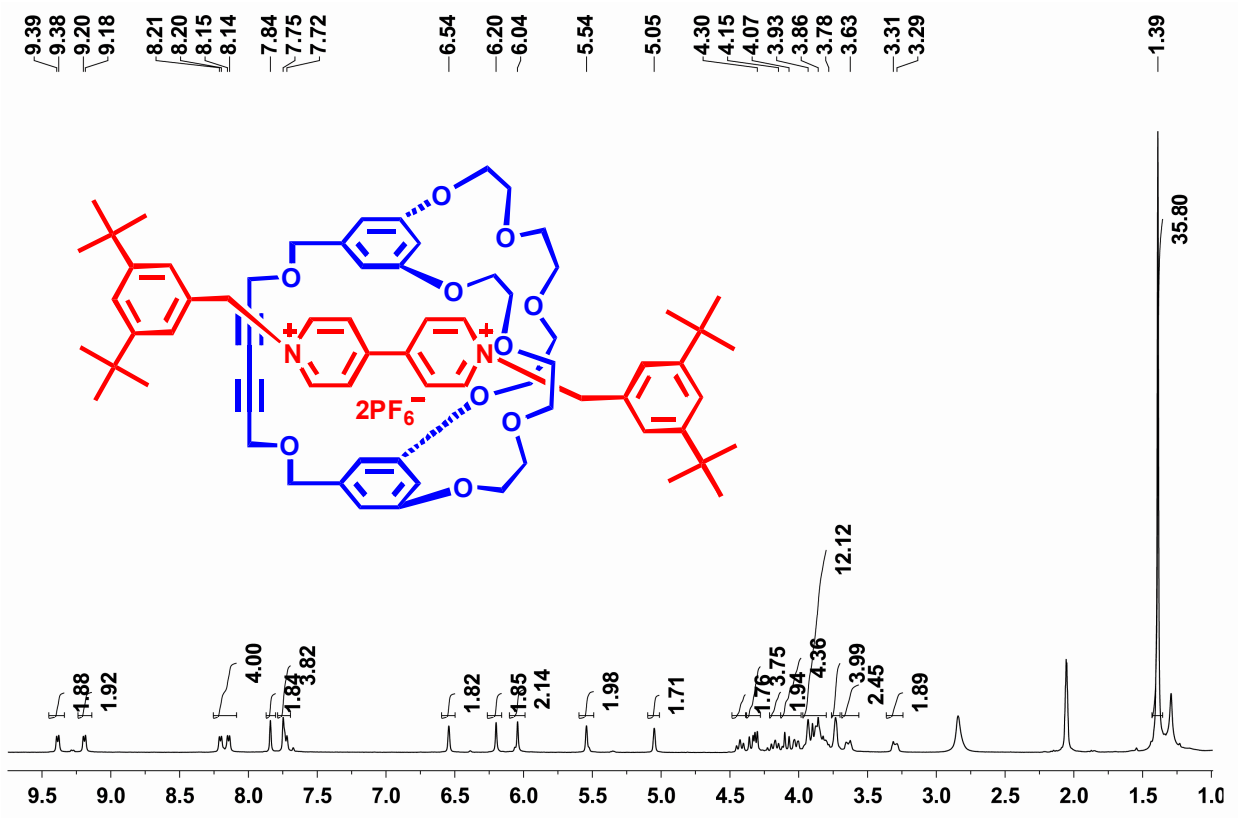

Figure S8 ^{1}H NMR spectrum (400MHz, CD_3COCD_3, 22℃) of [2]rotaxane **7**

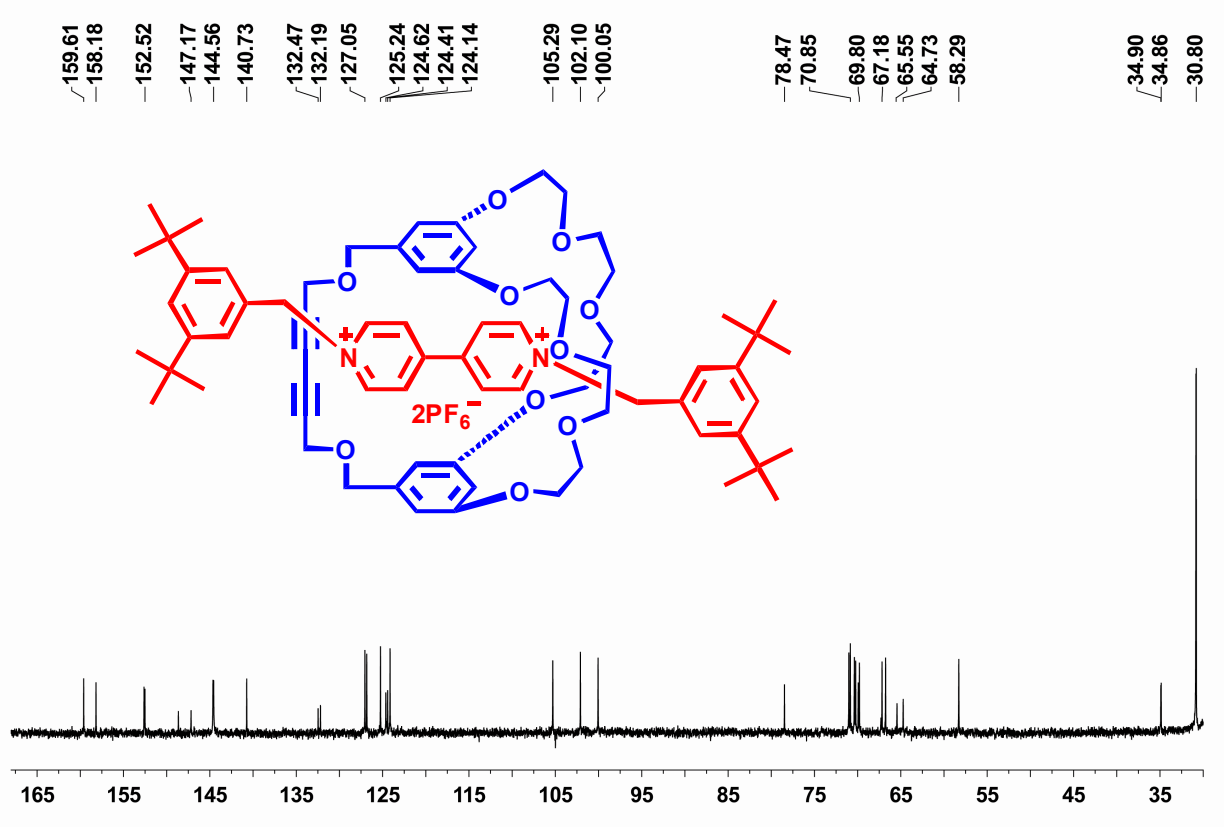

Figure S9 ^{13}C NMR spectrum (100MHz, CD_3COCD_3, 22℃) of [2]rotaxane **7**

6. Low- and high-resolution electrospray ionization mass spectra of [2]rotaxane **7**

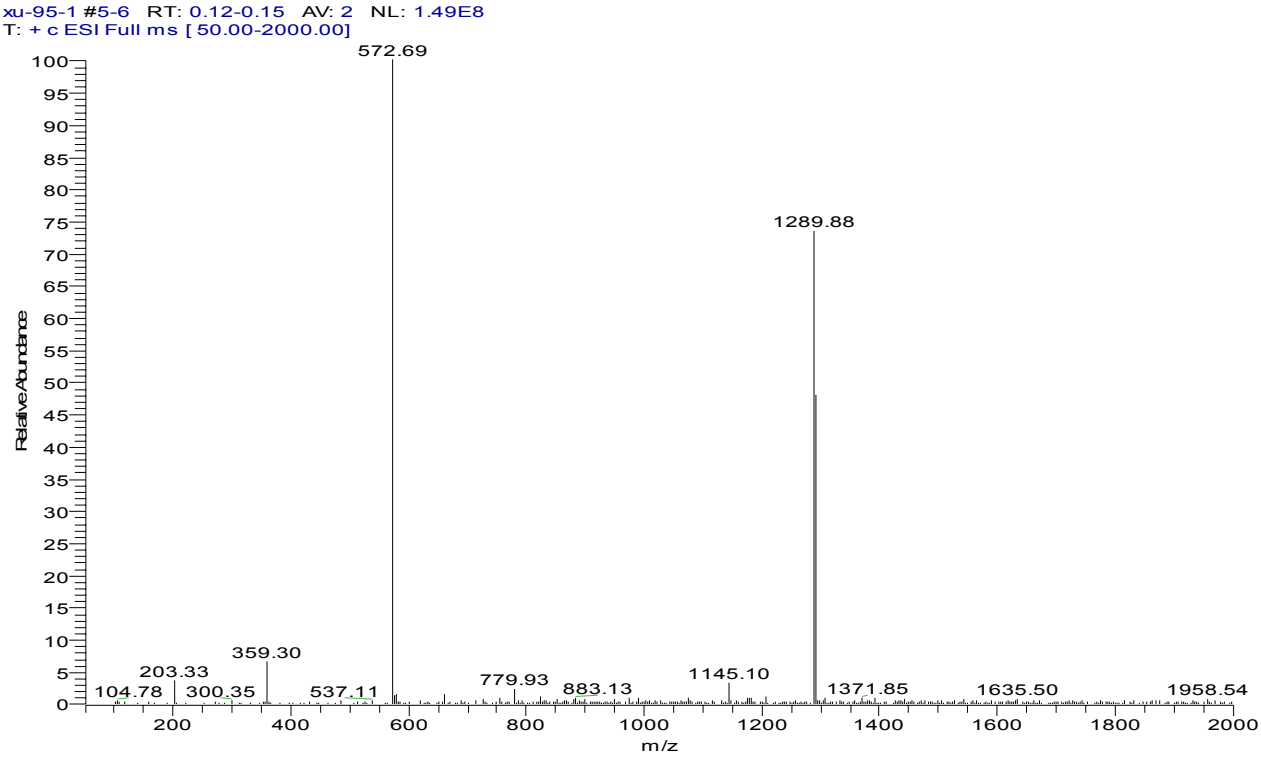

Figure S10 Low-resolution ESI-MS of [2]rotaxane **7**

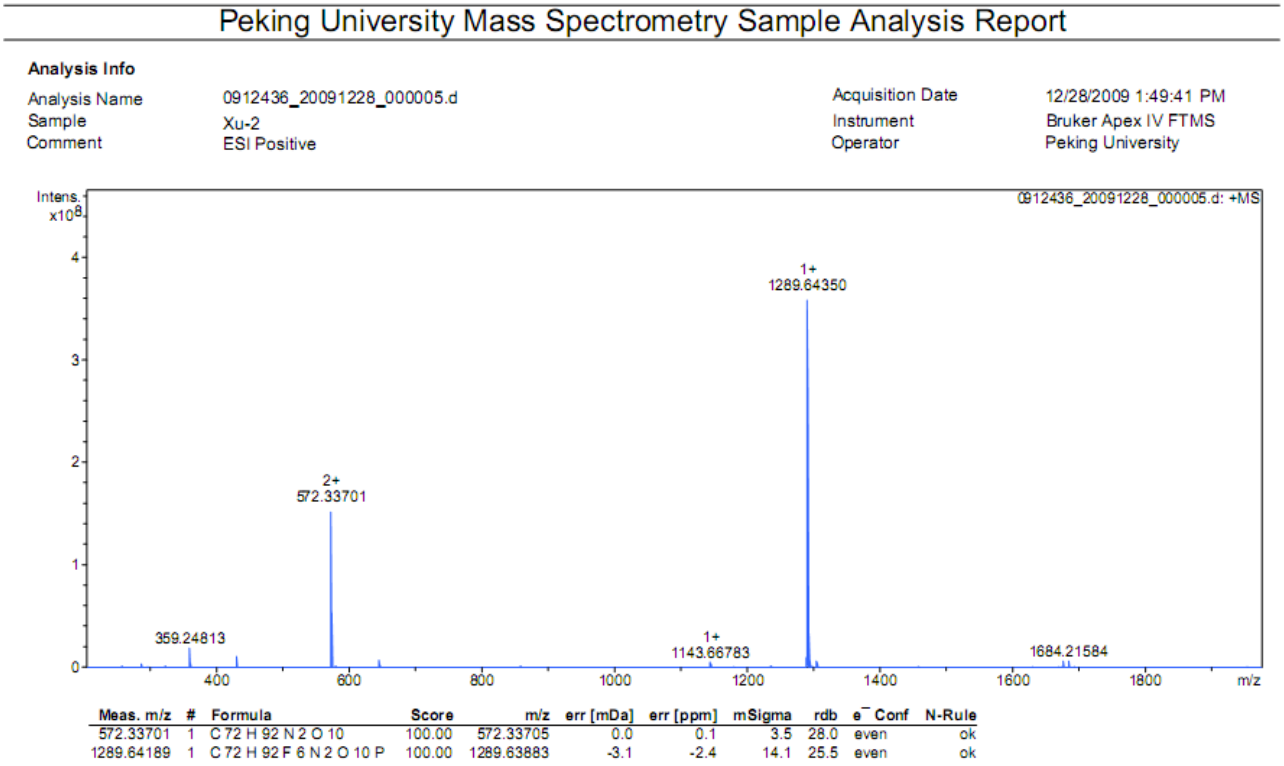

Figure S11 High-resolution ESI-MS of [2]rotaxane **7**

7. ^{1}H NMR and ^{13}C NMR spectra of [2]rotaxane **8**

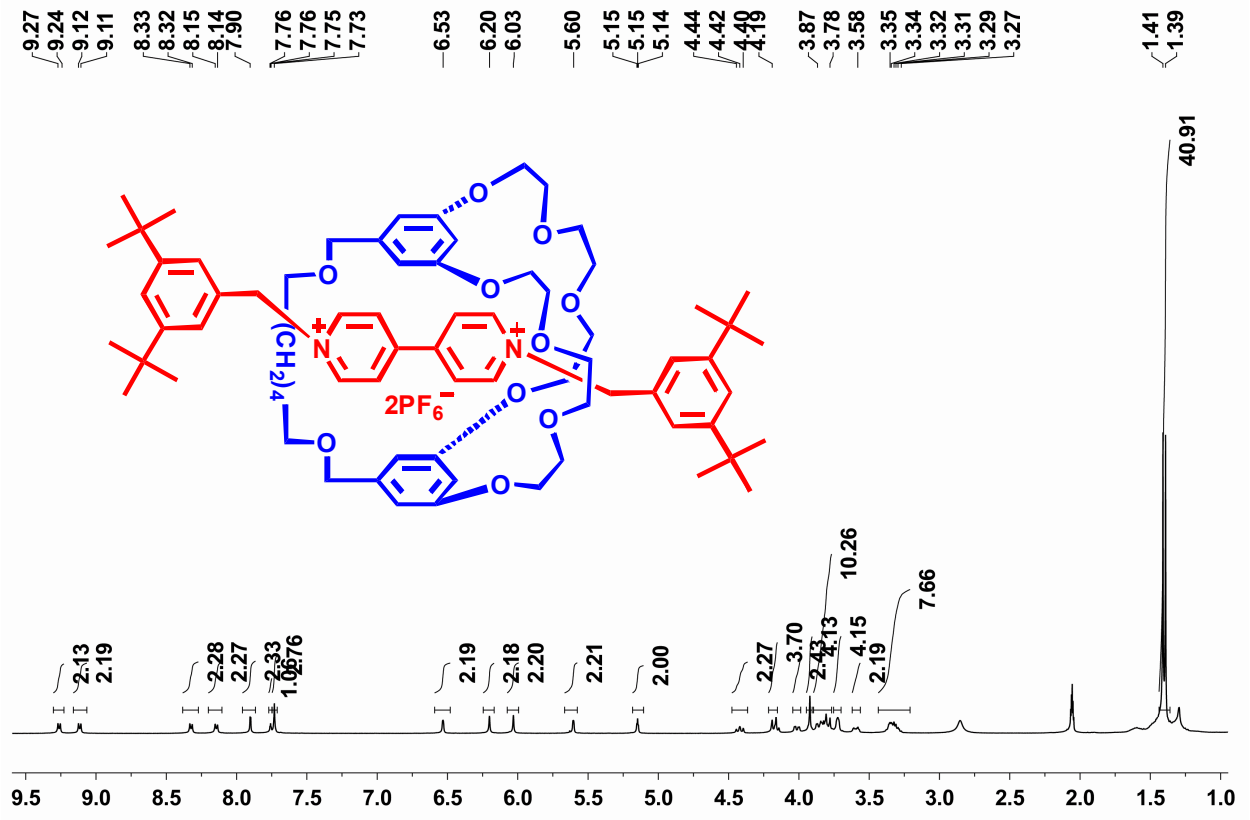

Figure S12 ^{1}H NMR spectrum (400MHz, CD_3COCD_3, 22℃) of [2]rotaxane **8**

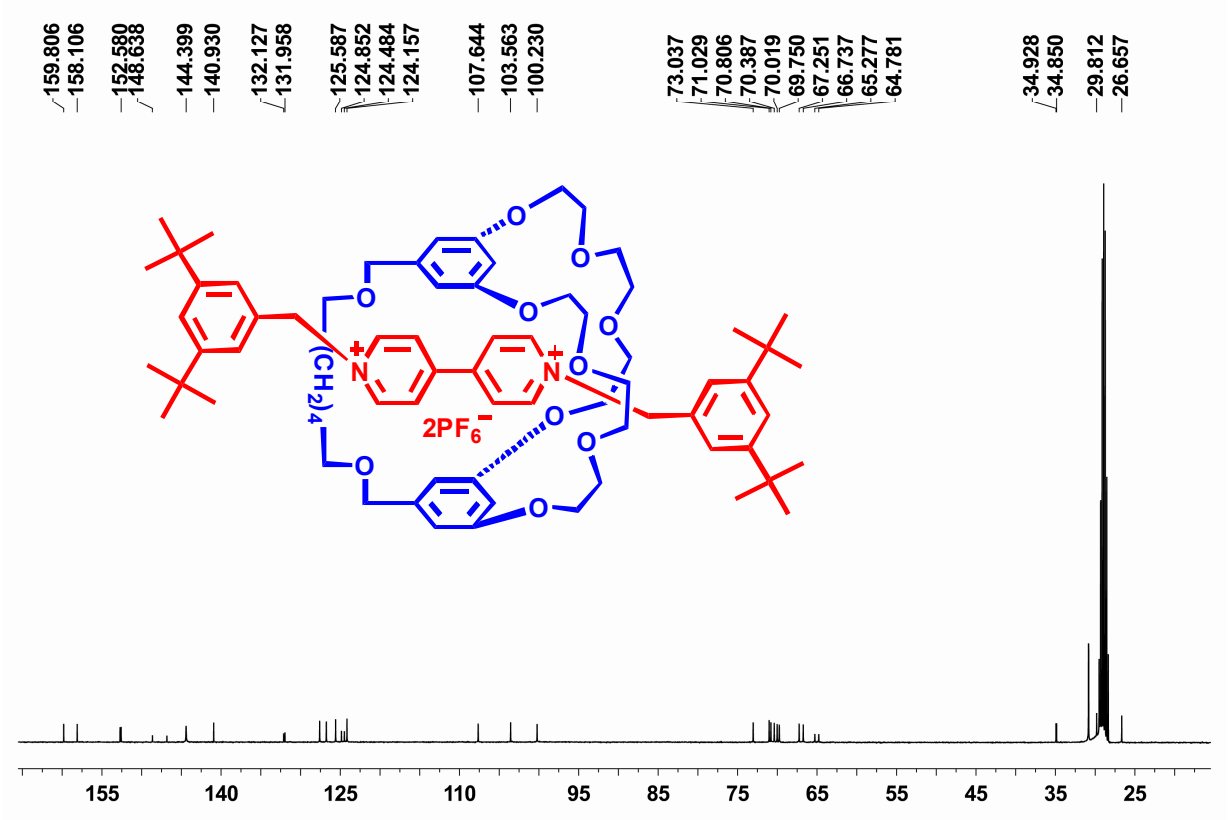

Figure S13 ^{13}C NMR spectrum (100MHz, CD_3COCD_3, 22℃) of [2]rotaxane **8**

8. Low- and high-resolution electrospray ionization mass spectra of [2]rotaxane **8**

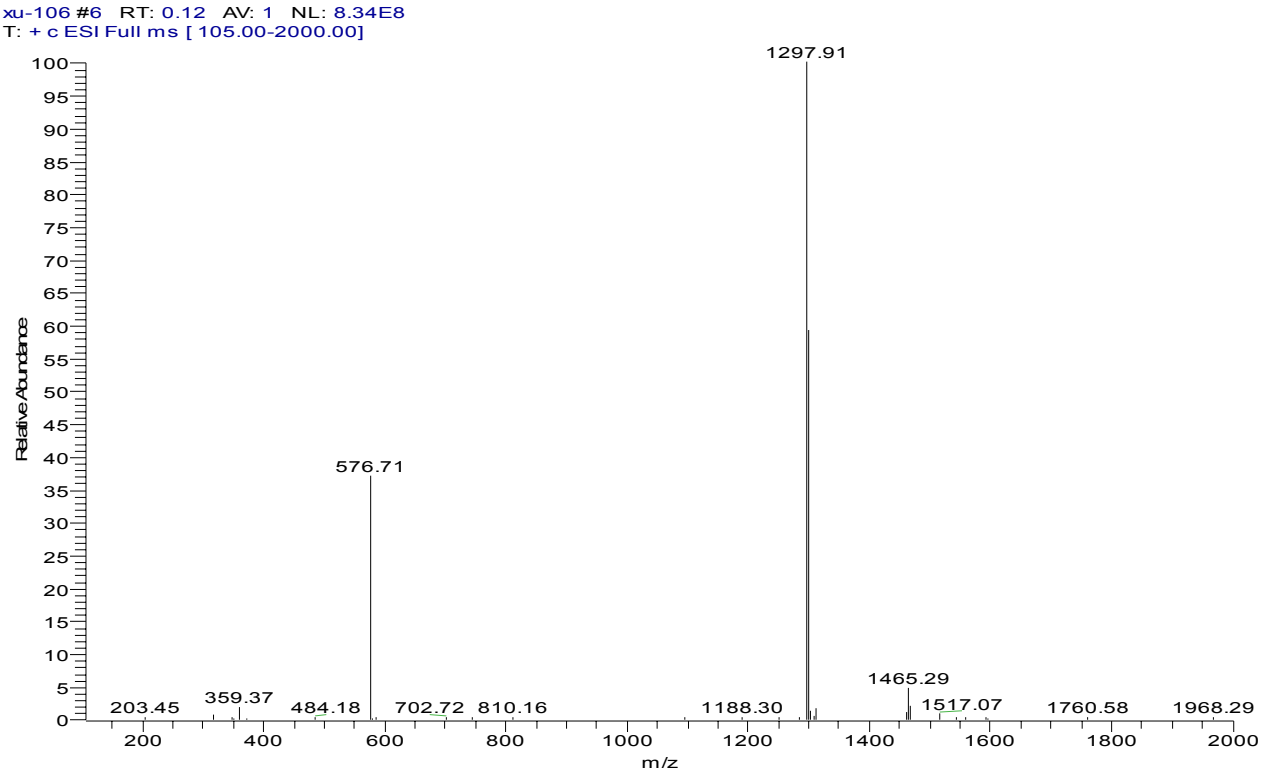

Figure S14 Low-resolution ESI-MS of [2]rotaxane **8**

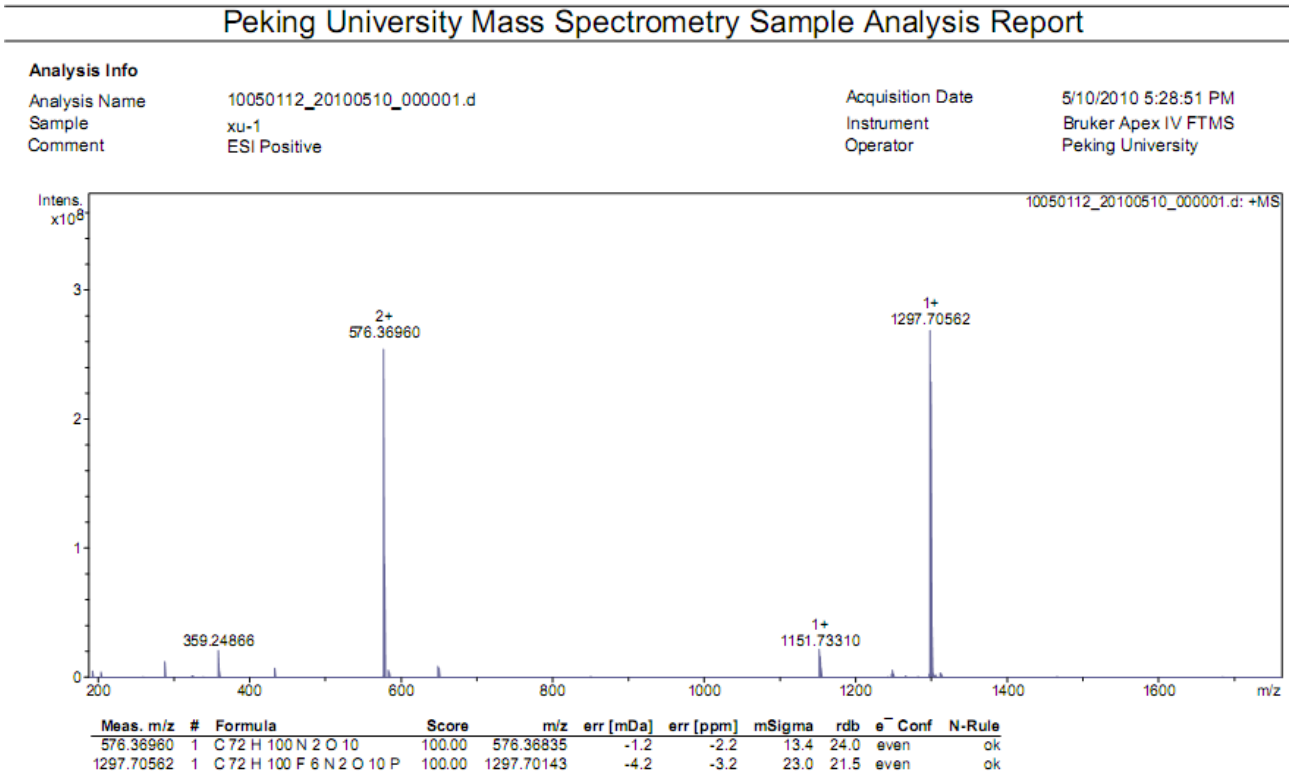

Figure S15 High-resolution ESI-MS of [2]rotaxane **8**

9. ^{1}H-^{1}H COSY and ^{13}C-^{1}H COSY spectra of [2]rotaxane **7**

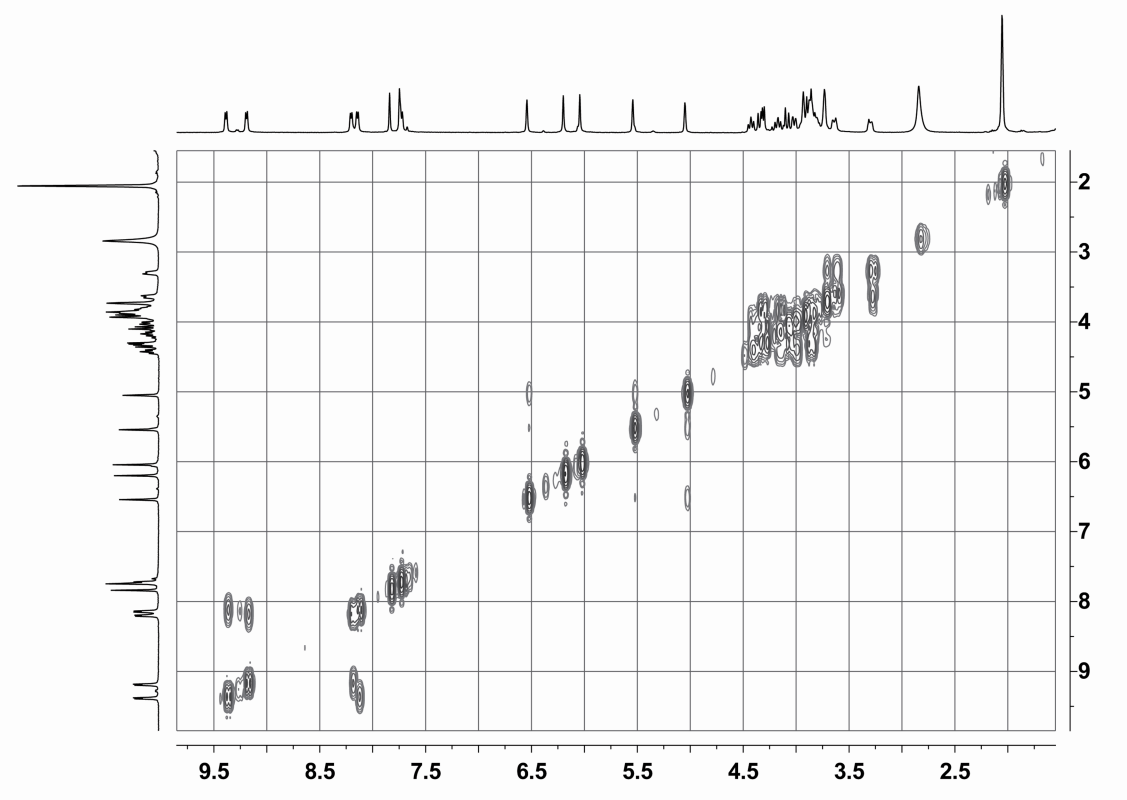

Figure S16 ^{1}H-^{1}H COSY spectrum (400MHz, CD_3COCD_3, 22℃) of [2]rotaxane **7**

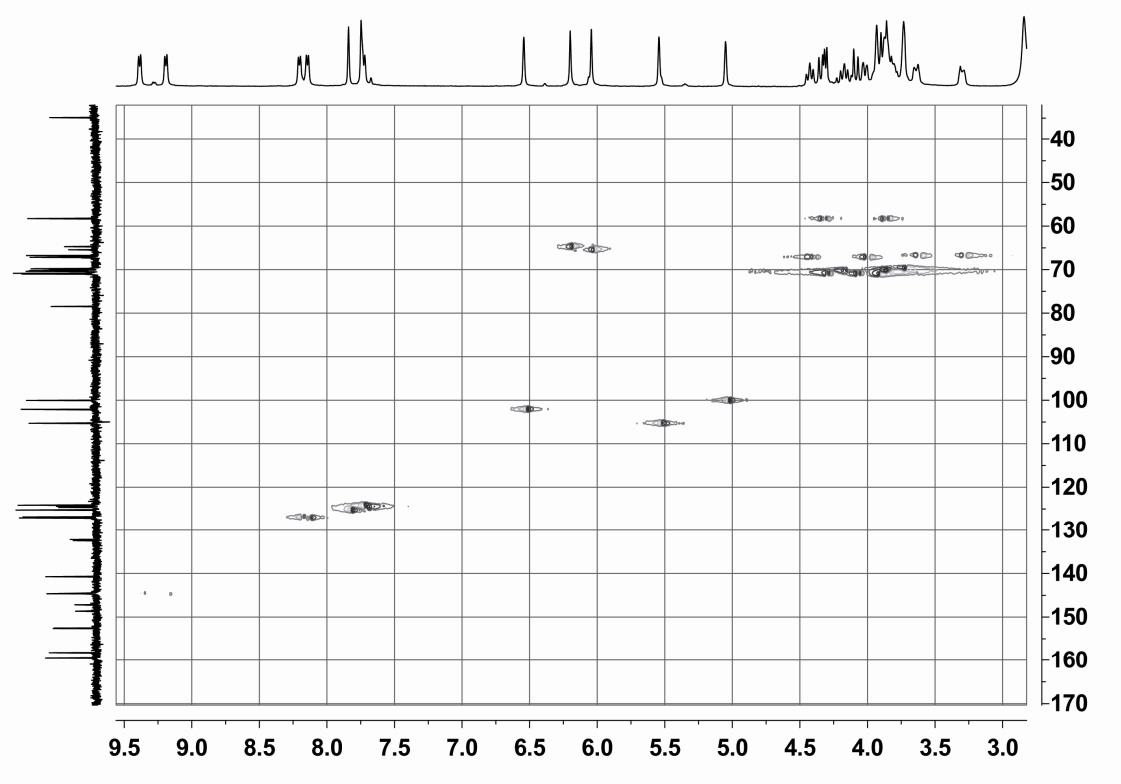

Figure S17 ^{13}C-^{1}H COSY spectrum (400MHz, CD_3COCD_3, 22℃) of [2]rotaxane **7**

10. ^{1}H-^{1}H NOESY and ^{13}C-^{1}H HMQC spectra of [2]rotaxane **7**

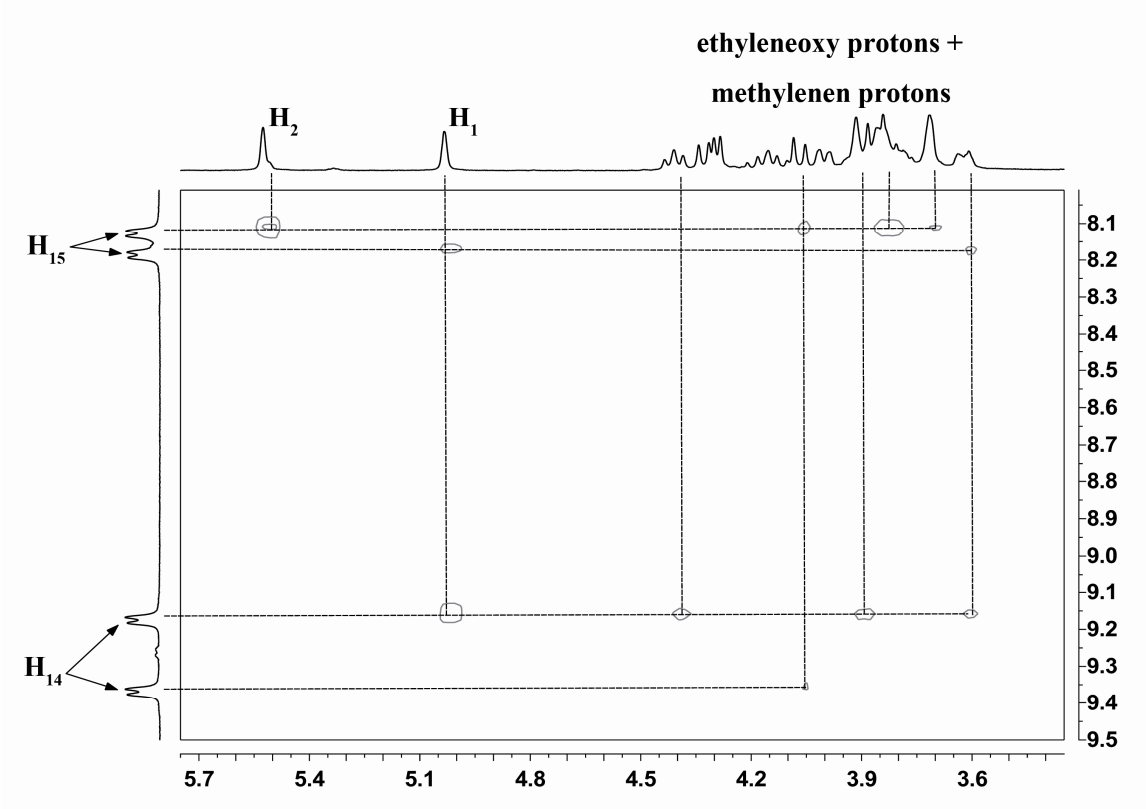

Figure S18 ^{1}H-^{1}H NOESY spectrum (400MHz, CD_3COCD_3, 22℃) of [2]rotaxane **7**

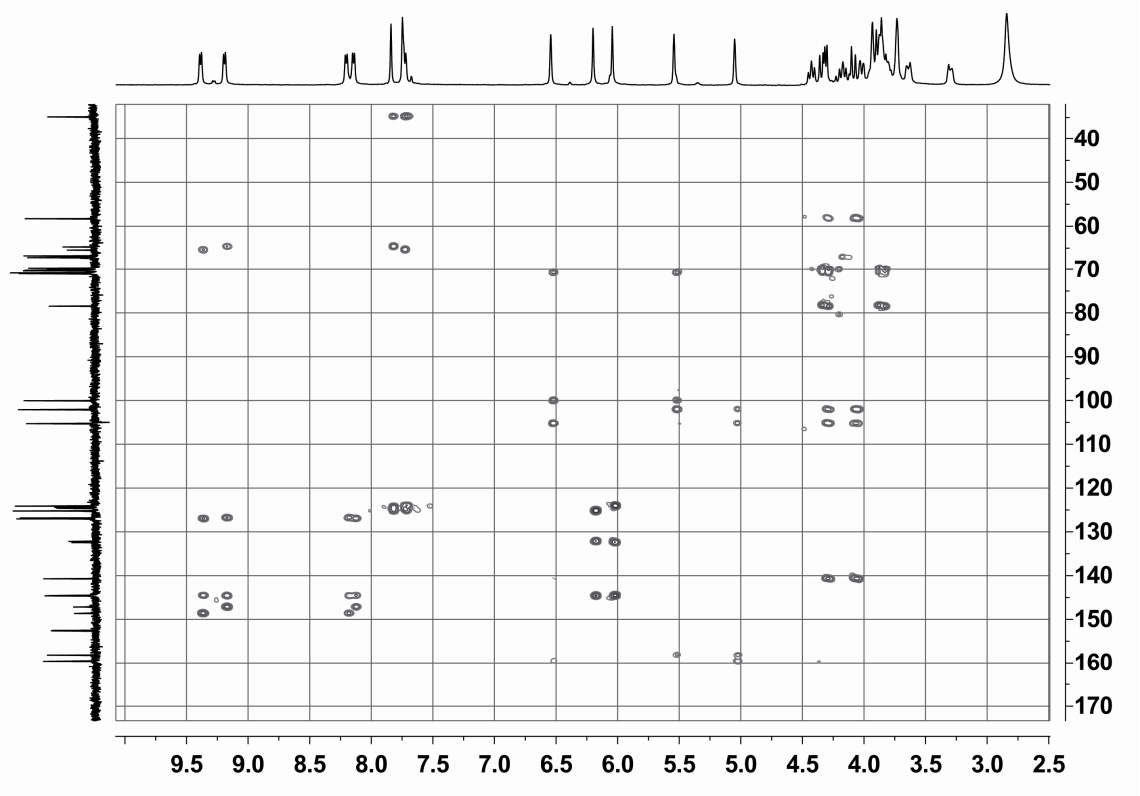

Figure S18 ^{13}C-^{1}H HMQC spectrum (400MHz, CD_3COCD_3, 22℃) of [2]rotaxane **7**

11. ^{1}H-^{1}H COSY and ^{13}C-^{1}H COSY spectra of [2]rotaxane **8**

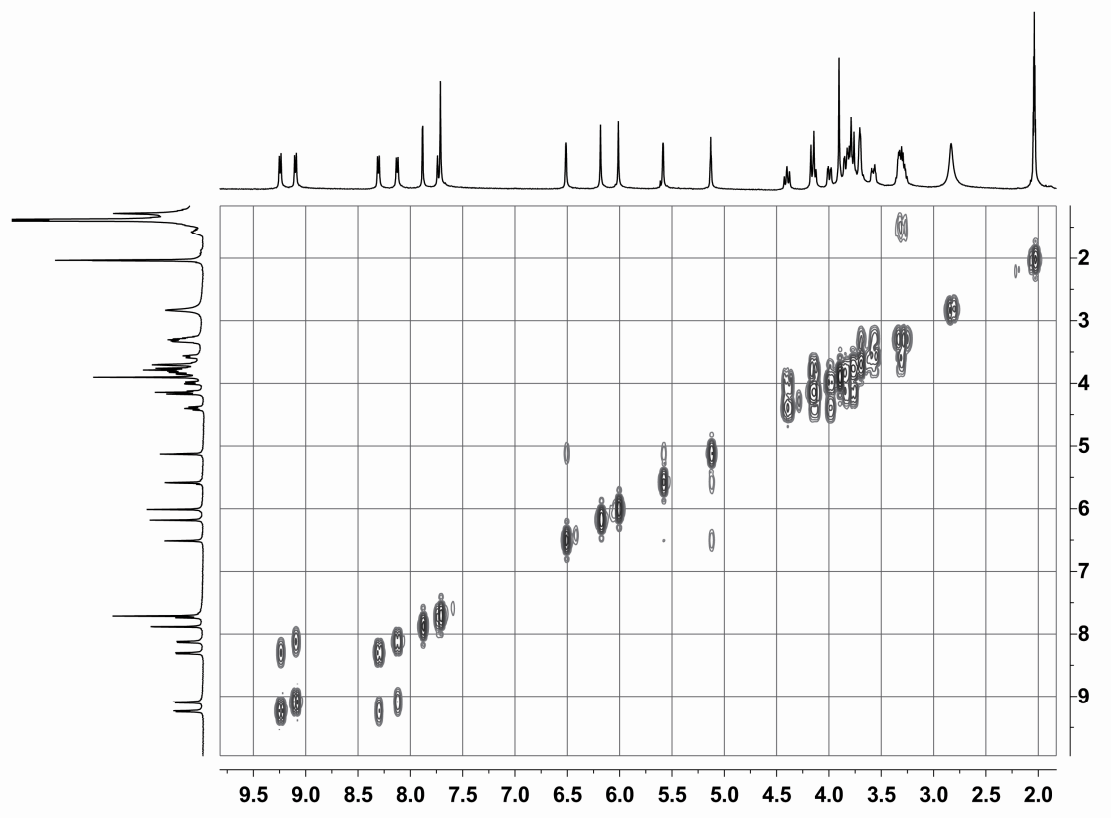

Figure S20 ^{1}H-^{1}H COSY spectrum (400MHz, CD_3COCD_3, 22℃) of [2]rotaxane **8**

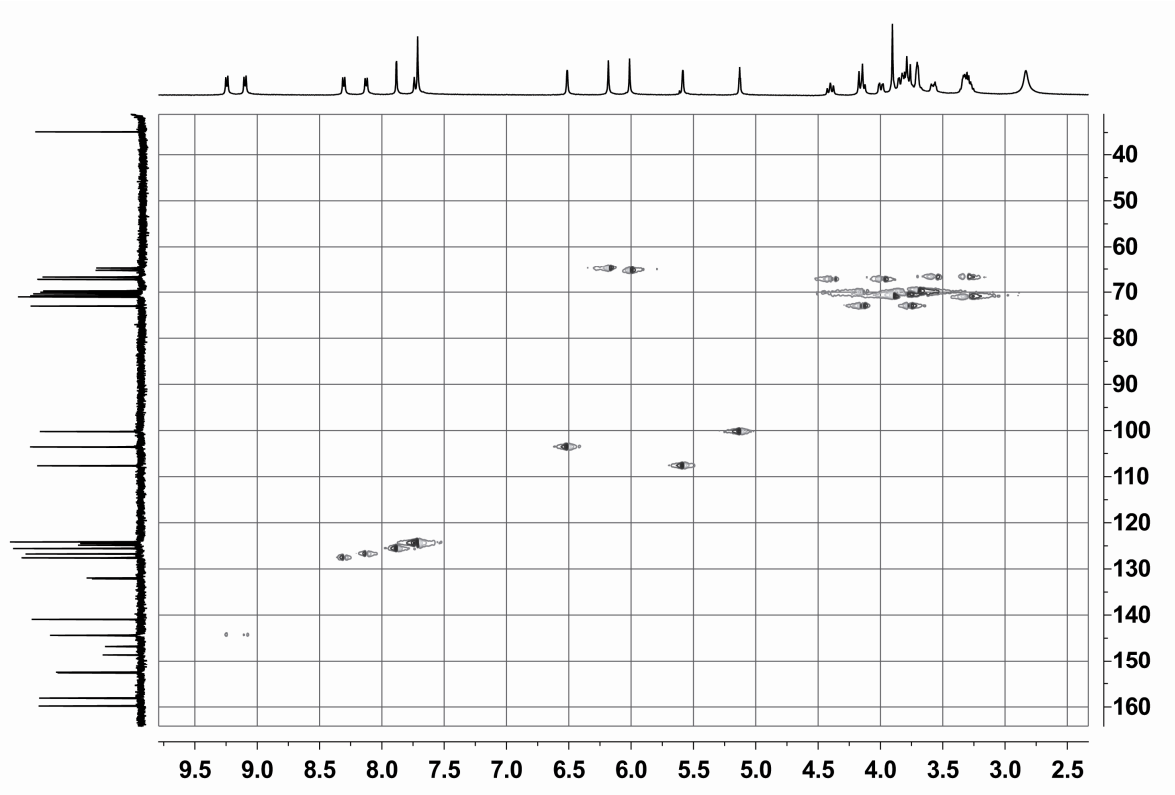

Figure S21 ^{13}C-^{1}H COSY spectrum (400MHz, CD_3COCD_3, 22℃) of [2]rotaxane **8**

12. ^{1}H-^{1}H NOESY and ^{13}C-^{1}H HMQC spectra of [2]rotaxane **8**

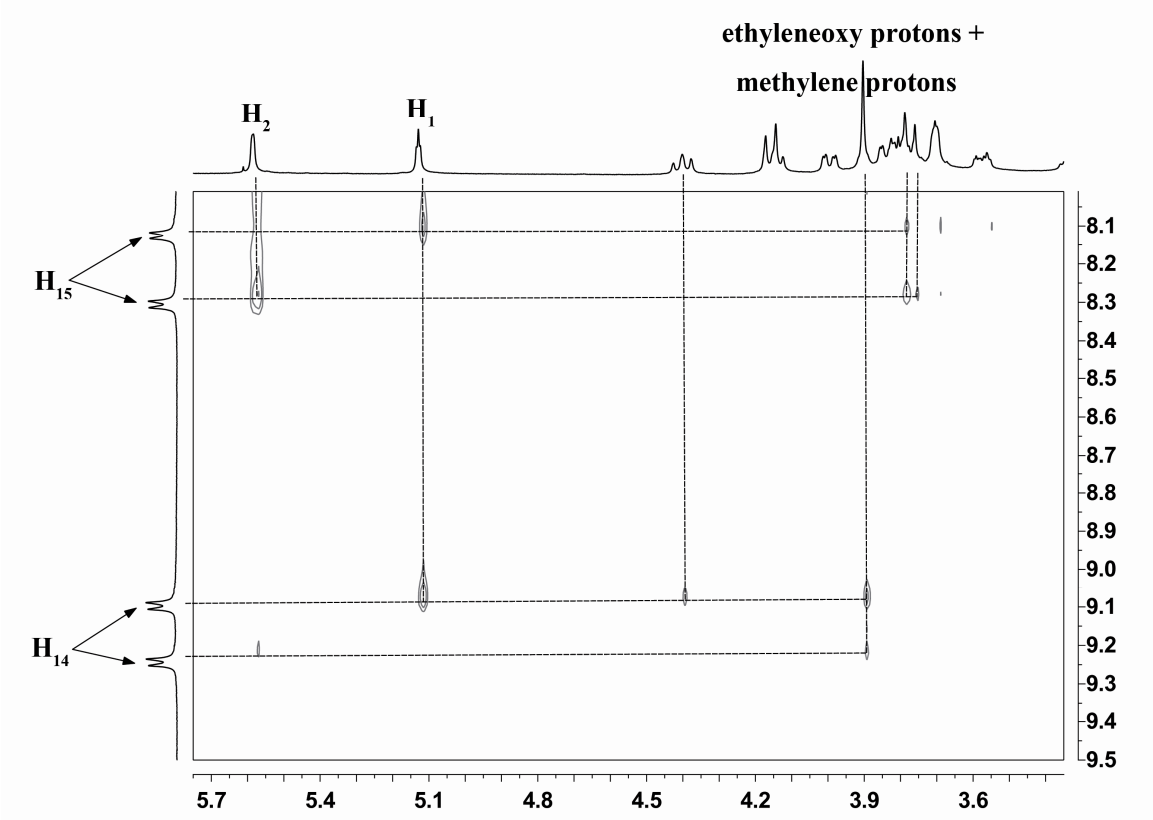

Figure S22 ^{1}H-^{1}H NOESY spectrum (400MHz, CD_3COCD_3, 22℃) of [2]rotaxane **8**

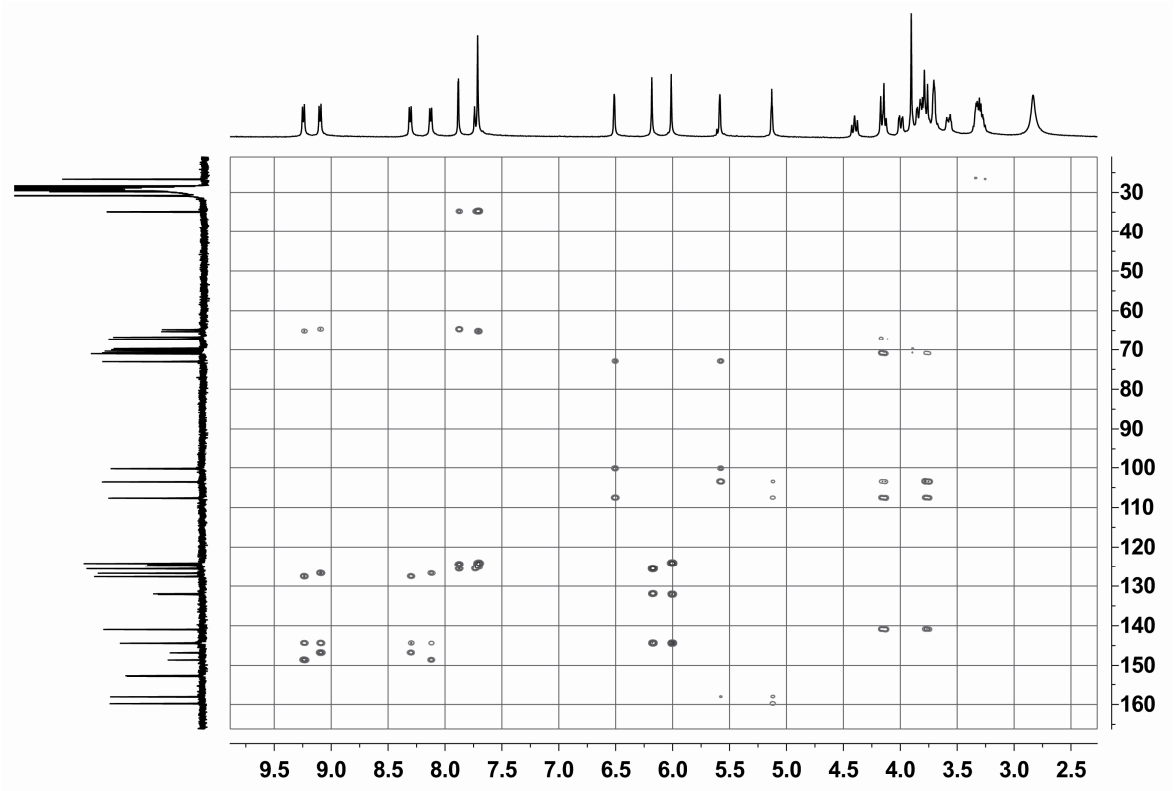

Figure S23 ^{13}C-^{1}H HMQC spectrum (400MHz, CD_3COCD_3, 22℃) of [2]rotaxane **8**

13. UV-Vis absorption spectra of cryptand **1a**, cryptand **1b**, dumbbell-shaped component **6**, [2]rotaxane **7** and [2]rotaxane **8**

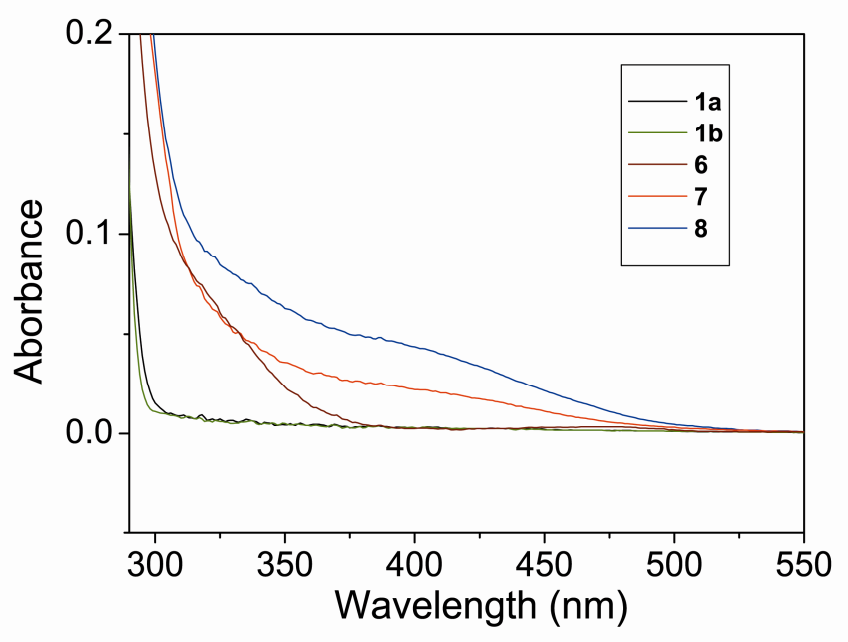

Figure S24 The UV-Vis absorption spectra of cryptand **1a**, cryptand **1b**, dumbbell-shaped component **6**, [2]rotaxane **7** and [2]rotaxane **8** at room temperature in acetonitrile ($[C]_0 = 5.0*10^{-5}$ M).

14. X-ray analysis data of [2]pseudorotaxane **1a·3**

X-ray analysis data of [2]pseudorotaxane 1a·3: Crystallographic data: block, pale red, 0.35×0.21×0.11 mm^3, $C_{56}H_{60}F_{12}N_2O_{10}P_2$, FW 1211.00, Monoclinic, space group $P2_1/c$, a = 12.789(3), b = 26.622(6), c = 20.717(4) Å, α = 90.00, β = 127.862(10), γ = 90.00° , V = 5569(2) $Å^3$, Z = 4, D_c = 1.444 $g·cm^{-3}$, T = 293(2) K, μ = 0.178 mm^{-1}, 28408 measured reflections, 10036 independent reflections, 739 parameters, 0 restraints, $F(000)$ = 2512, R_1 = 0.2044, wR_2 = 0.3405 (all data), R_1 = 0.0974, wR_2 = 0.2718 [$I > 2\sigma(I)$], max. Residual density 0.612 $e·Å^{-3}$, goodness-of-fit (F^2) = 1.031.

15. X-ray analysis data of [2]pseudorotaxane **1b·3**

X-ray analysis data of [2]pseudorotaxane 1b·3: Crystallographic data: block, pale red, 0.48×0.24×0.11 mm^3, $C_{56}H_{68}F_{12}N_2O_{10}P_2$, FW 1219.06, Triclinic, space group P-1, a= 13.672(11), b = 14.541(11), c = 16.402(12) Å, α = 112.152(10), β = 92.063(12), γ = 104.255(12)° , V = 2897(4) $Å^3$, Z = 2, D_c = 1.398 $g·cm^{-3}$, T = 298(2)K, μ = 0.172 mm^{-1}, 15071 measured reflections, 10446 independent reflections, 739 parameters, 0 restraints, $F(000)$ = 1272, R_1 = 0.3528, wR_2 = 0.3432 (all

data), R_1 = 0.1022, wR_2 = 0.2318 [$I > 2\sigma(I)$], max. Residual density 0.486 e·Å^{-3}, goodness-of-fit (F^2) = 0.949.

The level A alerts in [2]pseudorotaxane **1b·3** was due to small size of the crystal, which resulted in weak diffraction. We tried our best, including growing crystals in different solvent systems and performing data collection on different single crystals, but no better data set could be obtained.

16. X-ray analysis data of [2]rotaxane **7**

X-ray analysis data of [2]rotaxane 7: Crystallographic data: block, yellow, 0.68×0.35×0.21 mm^3, $C_{72}H_{92}F_{12}N_2O_{11}P_2$, FW 1451.42, Monoclinic, space group $P2_1/c$, a= 13.677(3), b = 17.347(4), c = 34.994(7) Å, α = 90.00, β = 106.807(7), γ = 90.00° , V = 7922(3) Å^3, Z = 4, D_c = 1.217 g·cm^{-3}, T = 298(2)K, μ = 0.137 mm^{-1}, 73478 measured reflections, 13959 independent reflections, 955 parameters, 384 restraints, F(000) = 3056, R_1 = 0.2379, wR_2 = 0.5147 (all data), R_1 = 0.1610, wR_2 = 0.4757 [$I > 2\sigma(I)$], max. Residual density 0.910 e·Å^{-3}, goodness-of-fit (F^2) = 1.717.

The crystal data of [2]rotaxane **7** is not well. The relatively high R_1, wR_2 and F^2 was attributed to the disorder of *tert*-butyl group. All attempts to obtain better quality crystals failed. Although the present crystal data is not good, the framework can be clearly solved and the crystallographic data strongly supports the spectroscopic characterizations.